

A progress report for the Latvian Council of Science project conducted within the Fundamental and applied research projects framework “*Engineered surface platform for immobilization of microorganisms*” (Izp-2018/1-0460) on the work done during the 01.09.2018. – 01.12.2019. time frame

The report includes progress information on the following tasks:

- Sample irradiation with UV light under controlled environment conditions and subsequently performed cell immobilization studies using the irradiated samples.

Achieved results

Cell deposition was performed on 4 samples from 4 groups of micropatterned samples which were (1) 39-1-6 (exposed for 30 minutes), (2) 39-1-6 (exposed for 30 minutes), (3) 39-1-6 (exposed for 60 minutes) and (4) 39-1-10 (exposed for 60 minutes). 16 samples were used in total. Samples were used immediately after exposure to UV radiation. Deposition was performed simultaneously for all samples, thus two Petri’s with two sample holders were used. Sample imaging was performed as was previously described in Progress report 3, only this time the number of acquired images was 2304 and the number of images considered for analysis was 1600.

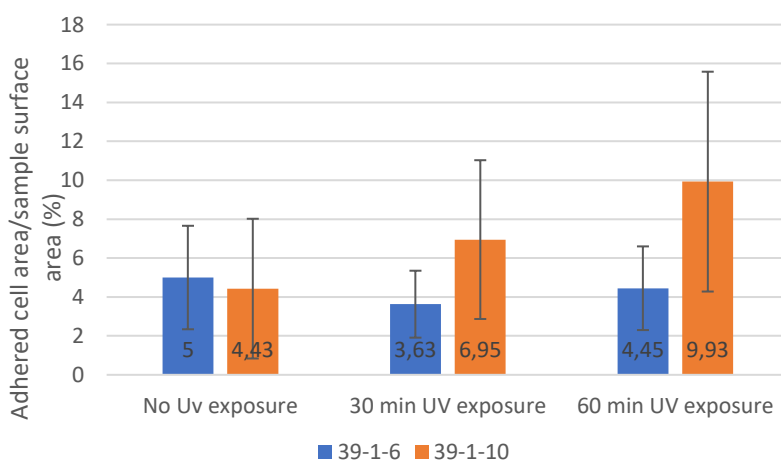


Figure 1. Changes in adhered cell count in relation to UV exposure time.

For 39-1-6 and 39-1-10 samples that were exposed to UV radiation for 30 minutes the cell/surface ratio was $3.63 \pm 1.72\%$ and $6.95 \pm 4.08\%$, respectively. For 39-1-6 and 39-1-10 samples that were exposed to UV radiation for 60 minutes the cell/surface ratio was $4.45 \pm 2.15\%$ and $9.93 \pm 5.65\%$, respectively. The data shows two possible trends for the change in the amount of cells adhered to a samples surface in response

to exposure to UV light: a) for 39-1-6 samples the change in the amount of cells with dose changes similarly to the change in surface potential for plateaus with a minimum at 30 minutes and a rising value at 60 minutes, b) for 39-1-10 samples the change is similar to the change in surface potential for valleys with a constant increase in attached cells with increase in exposure time. A graphical representation of the data can be seen in Figures 1, 2 and 3. The newly acquired data were compared with the previously acquired data for cells deposited on non-irradiated samples.

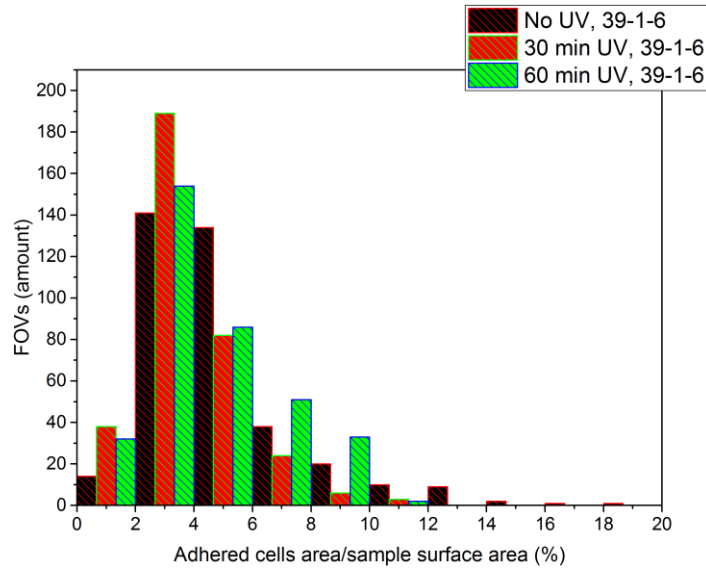


Figure 2. Distribution of cell/surface ratios of all valid FOVs taken from exposed and non-exposed 39-1-6 samples.

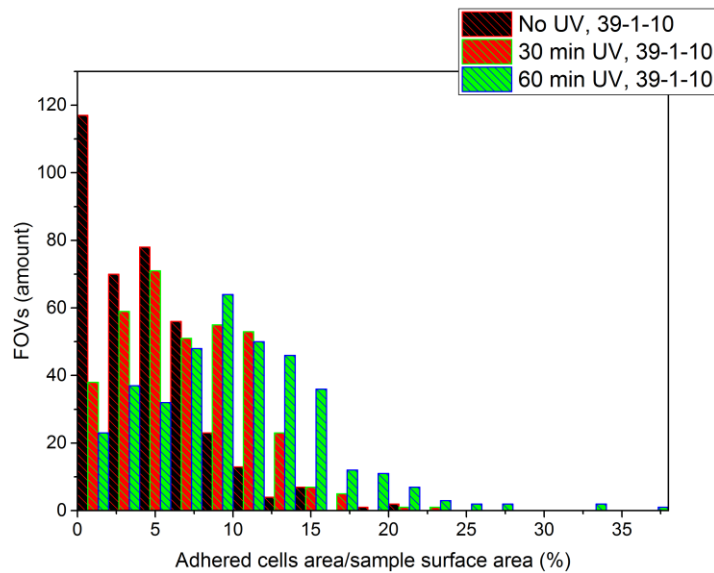


Figure 3. Distribution of cell/surface ratios of all valid FOVs taken from exposed and non-exposed 39-1-10 samples.

In Progress report 3 it was suggested that a different, more precise cell area counting algorithm should be developed. Therefore, a new and improved algorithm has been developed. However, at the moment it was used only on images acquired from samples that did not undergo exposure to UV light.

Since the images contain a periodic array of structures which is the same in every point on the samples surface it becomes possible to compare two images – one with cells deposited onto the surface and one that didn't undergo cell deposition – to then mark the areas that differ in color. First a mask was created using images from a sample that didn't undergo cell deposition. Since the images taken using the custom-made motorized stage are a little bit skewed, i.e. the sides of the structures aren't parallel to the edge of the image, they need to be rotated and then an area of the image that had only whole structures (edge structures tended to not be fully present in the image) needed to be cut out. Therefore, the image that was selected to serve as a mask was first rotated so that the structure sides are parallel to the edge and then a region of the image containing only whole structures was cut out. The dimensions of the resulting masks were 1506x1090 pixels² for 39-1-10 samples and 1393x1043 pixels² for 39-1-6 samples.

Using MATLABs image processing functionality, the mask image was manually overlaid on top of a pre-rotated image of a surface that underwent cell deposition (will be referred to as "target") so that the structures are located strictly on top of one another. Here as well only areas with whole structures were considered. After confirming the position of the overlay an image was cut out from the target which was then automatically compared to the mask.

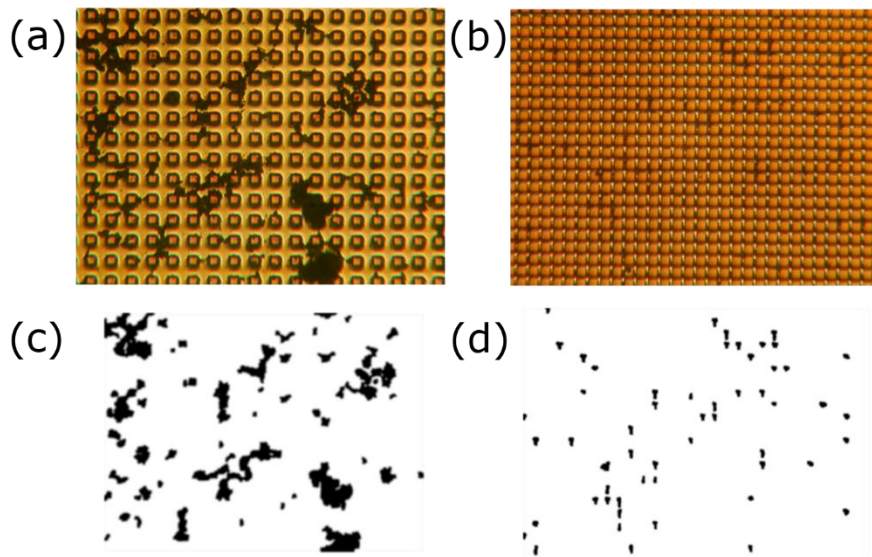


Figure 4. Image samples of FOVs used during analysis: (a), (c) image of a 39-1-6 sample before and after processing with the new algorithm, respectively; (b), (d) image of a 39-1-10 sample before and after processing with the new algorithm, respectively.

The cropped target and the mask images were converted into grayscale and then combined into one using MATLABs `imfuse(cropped target, mask, 'falsecolor')` function (the text in parenthesis are the parameters used during processing). The resulting image was then converted into HSV color units and the saturation channel was selected for processing. The image was converted into black and white using the `im2bw(saturation, 0.68)`. Features smaller than 100 pixels² (<6.76 mkm²) were visually identified as debris and were removed using `bwareaopen(black & white, 100)`. Area underselection was compensated by using dilation through `imdilate(black & white, strel('disk', 5))`. This approach allowed to create a two-color image with regions of the target that are similar to the mask colored black and regions of the target distinct from the mask colored white. These white regions are the areas where cells got attached to the surface. Finally, the area taken up by the now white-colored cells was counted using the `bwlabel(black & white)` function and exported into a text document.

This algorithm was applied only to those images that had within them 16x12 whole microstructures for 39-1-6 samples and 29x21 whole microstructures for 39-1-10 samples. Thus, images from the edge of the sample had to be excluded from analysis. During the project this algorithm is planned to undergo validation and update, and the edge areas will be tabulated as well. Also, images that had damaged areas or contained large debris particles were excluded from analysis. Figure 4 provides sample images before and after processing.

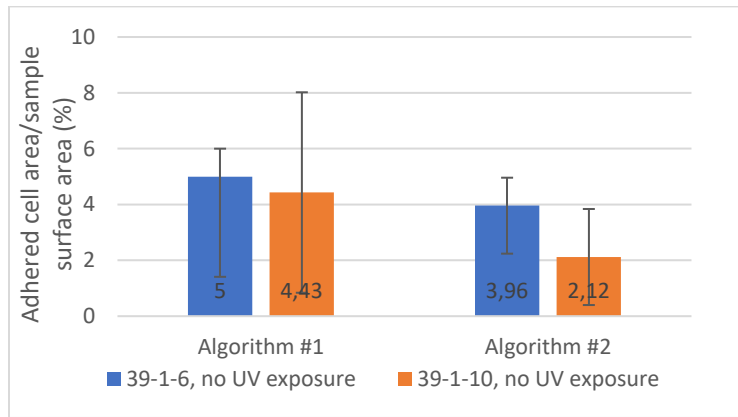


Figure 5. Average cell/surface ratio value comparison of FOVs processed using Algorithms #1 and #2.

This algorithm performed better than the first one in terms of cell marking. It was possible to use this algorithm without any alterations to its functionality on both 39-1-6 and 39-1-10 samples. For non-exposed 39-1-6 samples the cell/surface ratio was $3.96 \pm 1.86\%$ and for non-exposed 39-1-10 samples the ratio was $2.12 \pm 1.72\%$. A comparison of the values acquired using the improved algorithm with the ones acquired from the same images using the initial algorithm are given in Figure 5. A decrease in values for data processed using the improved algorithm can be seen. No noticeable change in the “standard deviation/value” ratio occurred for samples from group 39-1-10 and a 6% decrease in the value of this ratio occurred for samples from group 39-1-6. Histograms depicting the value distribution for the cell/area ratio are given in Figure 6.

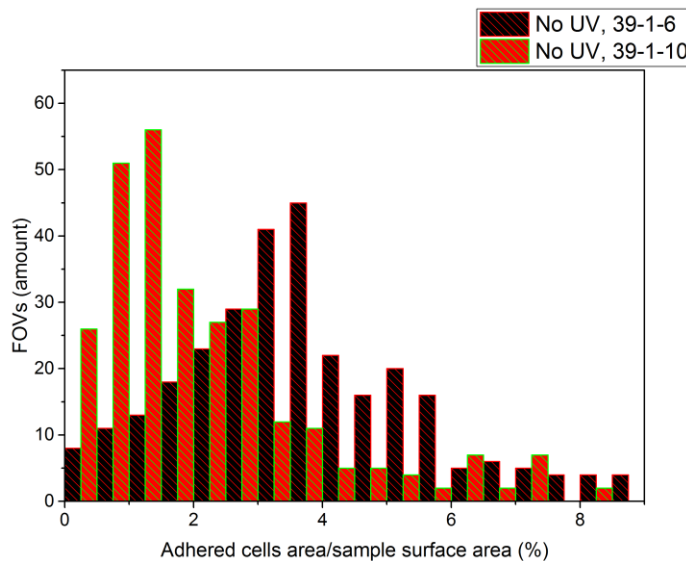


Figure 6. Distribution of average adhered cells/surface ratio values acquired using the improved algorithm.

Conclusion

Changes in surface potential of immobilization platform surfaces induced by exposing the samples to polychromatic UV light affect the way yeast cells attach to the sample; specifically, the amount of cells that become attached to the surface of a platform depends on the surface potential.